Nanomechanical and electrical properties of Nb thin films deposited on Pb substrates by pulsed laser deposition as a new concept photocathode for superconductor cavities

F Gontad, A Lorusso, M Panareo, A Monteduro, G Maruccio,
Esteban Broitman and A Perrone

Original Publication:

F Gontad, A Lorusso, M Panareo, A Monteduro, G Maruccio, Esteban Broitman and A Perrone, Nanomechanical and electrical properties of Nb thin films deposited on Pb substrates by pulsed laser deposition as a new concept photocathode for superconductor cavities, 2015, Nuclear Instruments and Methods in Physics Research Section A, (804), 132-136.
http://dx.doi.org/10.1016/j.nima.2015.09.064

Nanomechanical and electrical properties of Nb thin films deposited on Pb substrates by pulsed laser deposition as a new concept photocathode for superconductor cavities

F. Gontad[1,2], A. Lorusso[1,2,*], M. Panareo[1,2], A. G. Monteduro[1,2], G. Maruccio[1,2], E. Broitman[3], A. Perrone[1,2]

[1]*University of Salento, Department of Mathematics and Physics "E. De Giorgi", 73100 Lecce, Italy*

[2]*National Institute of Nuclear Physics, 73100 Lecce, Italy*

[3]*Thin Film Physics Division, IFM, Linköping University, 581-83 Linköping, Sweden*

[*]Corresponding author: Dr Antonella Lorusso; Tel.: +39 0832 297501; E-mail address: antonella.lorusso@le.infn.it

Abstract

We report a design of photocathode, which combines the good photoemissive properties of lead (Pb) and the advantages of superconducting performance of niobium (Nb) when installed into a superconducting radio-frequency gun. The new configuration is obtained by a coating of Nb thin film grown on a disk of Pb via pulsed laser deposition. The central emitting area of Pb is masked by a shield to avoid the Nb deposition. The nanomechanical properties of the Nb film, obtained through nanoindentation measurements, reveal a hardness of 2.8 ± 0.3 GPa, while the study of the electrical resistivity of the film shows the appearance of the superconducting transitions at 9.3 K and 7.3 K for Nb and Pb, respectively, very close to the bulk material values. Additionally, morphological, structural and contamination studies of Nb thin film expose a very low droplet density on the substrate surface, a small polycrystalline orientation of the films and a low contamination level. These results, together with the acceptable Pb quantum efficiency of 2×10^{-5} found at 266 nm, demonstrate the potentiality of the new concept photocathode.

KEY WORDS: Nb thin film, pulsed laser deposition, metallic photocathodes, superconductive radiofrequency cavity.

1. Introduction

The use of photoinjectors based on superconducting technology is an excellent choice for delivering electron beams of high average currents (> 1 mA) with near continuous wave and reduced power dissipation operation [1,2].

One of the most important challenges in the fabrication of photocathodes is the high quantum efficiency (QE) and their electrical compatibility with superconducting cavities (SC) technology usually made of niobium. Until now, no material has been found to satisfy these requirements, so it is necessary to make a compromise between both QE and electrical performance. The obvious solution to such a compromise is Pb, which presents a QE around 2×10^{-5} at 266 nm [3], much higher than Nb (7.4×10^{-7} at 266 nm [4]), which is a well-known superconductor with a superconducting transition temperature of 7.19 K and has a high chemical stability.

The feasibility of such lead photocathodes have been studied by mechanically incorporating into the Nb flange the Pb bulk material [1] or by depositing Pb thin film on the Nb flange surface through different deposition techniques, such as electroplated deposition, arc deposition, sputtering, evaporation [5] and pulsed laser deposition (PLD) [6,7].

Still, despite its remarkable chemical stability under vacuum conditions, lead photocathodes suffer from surface contamination upon exposure to atmospheric air conditions [6], requiring the use of superficial laser cleaning treatments prior to their normal operation. Unfortunately, such treatments may provoke delamination, consumption and also thinning of the photoemitting film, causing in turn a decrease of

the device performance and lifetime. In order to overcome such inconvenient, we propose a new configuration of superconducting photocathode in which a Pb disk is coated by a niobium film, except its central area that acts as the photo-emitting spot (Fig. 1), similar to the one proposed for conventional radiofrequency photoinjectors [7]. The use of the Pb bulk as the photoemitting material improves the response of the material to the laser cleaning processes, as the damage caused by such processes are minimized with respect to the case of photoemitting thin films, while the purpose of the Nb thin film is to reduce the surface resistance of the Pb bulk photocathode and, hence, to preserve the quality factor of the superconducting cavity.

The feasibility of superconductiong Nb yhin films in SC has been already tested on Cu [8] and MgO [9] substrates, while its deposition has been studied by DC magnetron sputtering [10], high-pressure magnetron sputtering [11], electron cyclotron resonance [12], low pressure chemical vapour deposition [13], molecular beam epitaxy [14], atomic layer deposition [15], coaxial energetic deposition [16] and e-beam evaporation [17].

In this work, we introduce the fabrication of new alternative Nb/Pb hybrid photocathode design through the deposition of Nb thin films on Pb substrates by PLD technique, with the ring configuration shown in figure 1. Their mechanical and electrical properties are evaluated in order to analyse their potentiality for their actual superconducting photocathode application.

2. Experimental procedures

All the deposition processes were performed in high vacuum (2.2×10^{-6} Pa) and at room temperature. The fourth harmonic of an Nd:YAG laser (Continuum, Powerlite Precision II-8010) (266 nm, 7 ns (FWHM) pulse duration and a repetition rate of 10 Hz) was focused onto the Nb target at an incidence angle of 45º using a 30 mm focal length quartz lens. In order to clean the target surface it was ablated with 2,000 pulses, while the transfer of the target material to the substrate surface was avoided by means of a shutter. After the target cleaning, the deposition was carried out with the cumulative effect of 60,000 laser pulses on three different tracks in order to avoid deep crater formation on the surface of the target which rotated with a frequency of 3 Hz. The ablated material was collected on Pb substrates kept at distance of 5 cm from the target surface. The laser fluence was optimized at 8.5 J/cm^2 after a parametric study [18]. The spot size of the laser beam on the surface of Nb was about 1.4 mm. The other experimental conditions used in this study are listed in table I.

The mass spectra of the vacuum chamber residual gases were recorded with a quadrupole mass spectrometer (Hiden Analytical HALO 201 RC) in order to optimize the quality of the vacuum used for the deposition. The deposited films were analyzed by scanning electron microscopy (SEM, mod. JEOL-JSM-6480LV), X-ray diffraction (XRD, mod. RIGAKU D/MAX ULTIMA) and nanoindentation (Triboindenter TI-950, Hysitron) to deduce the morphology, the structure and the mechanical properties, respectively. The temperature dependence of the film electrical resistivity was measured within the variable temperature insert of a cryogen free closed cycle superconducting magnet (Cryogenic LTD) operated with a CSW-71D compressor (Sumitomo Heavy industries, Ltd). A two terminal method was employed, with a yokogawa 7651 programmable DC source and a Standford Research SR570 preamplifier to read the

current. Finally, quantum efficiency (QE) measurements were carried out by a photodiode cell described in a previous work [6].

3. Results and discussion

Scanning electron microscope image shows a very smooth surface and almost free of droplets or particles (figure 2). This property is an important parameter for the improvement of the surface conductivity of the films. In the same figure, the edge of the film is easily observable. Figure 3 shows Energy-Dispersive X-ray spectroscopy (EDX) maps of the central part of the sample, where part of the substrate surface has been shielded during the deposition in order to create the photoemitting area of the photocathode (figure 4). All the maps were acquired with an electron energy of 15 keV. The dark area on the Nb map (in green) corresponds to the area where the Pb substrate surface was shielded during the deposition. On the other hand, the EDX map of Pb (yellow signal) comes into view also in the area of the Nb thin film because some x-rays come from the Pb bulk due to its small thickness (60 nm). The weak signal for this chemical species is due to the relatively high energy value of K_α and L_α respect to the electron energy in this analysis. The oxygen map (red signal) shows very low concentration of oxygen in the film (Nb) and in the substrate (Pb). This fact indicates that the careful control of the vacuum level and of vacuum quality by mass spectrometric investigations, before and during the experiment, allows the growth of low contamination Nb thin films through PLD.

The XRD analysis of the sample (figure 5) indicates that the grown film presents an amorphous structure, with only a small trace of the (110) crystalline planes of the bcc

network as a broad small peak located around 2θ = 38º suggests [19,20]. All the peaks shown in the XRD pattern can be attributed to the Pb underlying substrate except for that weak band at 38º. Despite the Pb substrate presents a preferential orientation along the (111) crystalline planes of the cubic network, typical of fcc metals [21], the Nb film seems to grow with a preferential orientation along the (110) crystalline planes, typical of bcc metals [22]. Therefore, the crystalline texture of the film is not related to that of the Pb substrate but to the bcc metallic character of Nb films [22]. However, the energy of the ablated species does not seem to be enough to produce large grains, as the broadness of the peak at 2θ = 38º illustrates. Moreover, the low number of counts arising from such contribution indicates a low crystalline fraction, evidencing the presence of a large amorphous phase. The absence of large crystals on the film is not yet clear, but will be studied in future works, analysing the influence of the substrate temperature [23] or photon energy in the crystalline structure of the film. The thickness and mechanical properties of the Nb film were measured by performing nanoindentations with penetration depths displacements spanning a range which exceeded the coating thickness. The raw data was then processed using the approach of Oliver and Pharr to calculate hardness values of the Nb+Pb system, and corrected for pile-up effects [24] (figure 6). In order to calculate the thickness and hardness of the Nb film, we have used the model of Korsunsky and Constantinescu [25] which predicts:

$$H_c = H_s + (H_f - H_s)/(1 + b \times t/t_f) \qquad (1)$$

where H_c, H_s, and H_f are the composite hardness, substrate hardness and film hardness, respectively, t is the penetration depth of the nanoindentation probe, t_f is the

film thickness and b is a factor depending on the indenter shape. In our experiments, the fitting parameters H_f, t_f and b are determined by fitting to the experimentally determined variation of H_c with t, while the value of H_s = 0.22 ± 0.01 GPa was measured directly on the uncoated substrate. The result of the fitting reveals that the Nb film has a thickness of 60 ± 5 nm and a hardness of 2.8 ± 0.3 GPa. The factor b for the Berkovich tip of 200 nm diameter resulted to be equal to 3. To the best of our knowledge, there are no publications reporting the nanoindentation hardness of pure Nb thin films deposited by PLD. Furthermore, very little information is available for the mechanical properties of pure Nb films deposited by other physical vapour deposition techniques. Zhao and Lai [26] reported a value of 7.10 ± 0.27 GPa for thin films deposited by magnetron sputtering (MS). Bemporad *et al.* [27] measured values of 2.59 ± 0.35 GPa for unbiased and 3.10 ± 0.58 GPa for biased MS films deposited on Cu substrates. Dispersion of the measured values between both publications can be directly linked to microstructural differences of their films, like film density and grain size, which affect the mechanical properties of the coatings [28]. Our results fall inside of range of values measured by Bemporad *et al.* [27].

An additional indication about the value of the Nb film thickness can be deduced from the nanoindentation load-displacement curves, as shown in figure 7. All nanoindentation measurements present a change in the slope when the probe has displaced about 60 nm from the surface. The decrease in the slope can be associated to the penetration into the Pb substrate, which is about 10 times softer than the Nb film.

The hardness feature of the Nb thin film is very important for reducing the scratches formation on the photocathode-flange surface which could be responsible of electrical discharges due to the high gradient of electric field in SC cavity.

Another important aspect for the targeted application is the evaluation of the film

electrical performance for its integration in superconducting cavities. Figure 8 shows the evolution of the sample resistance with the temperature below 20 K. Two clear steps can be distinguished in the curve at 9.3 K and 7.3 K, which are very close to the critical temperatures of Nb and Pb, reported in literature to be 9.26 K and 7.19 K respectively [29,30]. These features can be thus associated to two superconducting transitions superimposed to a series resistance from the interconnections.

Finally, the photoemission performance of the sample, without any chemical or physical treatment of the surface, showed a relatively high QE of about 2×10^{-5} at 266 nm. As naturally expected, the photoemitting behaviour of the Nb/Pb photocathode is strictly similar with the one expected from the Pb bulk.

4. Conclusions

In this work the feasibility of fabricating new hybrid Nb/Pb devices with application as photocathodes for superconducting radiofrequency guns has been demonstrated. The morphology of the deposited Nb metallic film, characterized by SEM, presented a very low droplet density, which makes them very interesting for such application. Nanomechanical characterization has shown the hardness feature of the 60 nm Nb films which is very important for reducing the scratches formation on the photocathode surface. In addition, the EDX analysis showed the goodness of PLD for the fabrication of the new design superconducting photocathodes, with an extremely low film oxidation during the growth process. Finally, despite the low crystalline fraction of the Nb film obtained through XRD, the measured critical temperature and low resistivity of the film indicated the usefulness of PLD for the fabrication of high quality Nb thin films.

Acknowledgements

This work was supported by Italian National Institute of Nuclear Physics (INFN). A. Lorusso acknowledges the support from the Italian MIUR through the project FIRB Futuro in Ricerca 2010 (RBFR12NK5K). Esteban Broitman acknowledges the Swedish Government Strategic Research Area in Materials Science on Functional Materials at Linköping University (Faculty Grant SFO-Mat-LiU # 2009-00971).

References

[1] J. Smedley, T. Rao. J. Sekutowicz, Phys. Rev. ST Accel. Beams 11 (2008) 013502.

[2] R. Barday, A. Burrill, A. Jankowiak, T. Kamps, J. Knobloch, O. Kugeler, A. Matveenko, A. Neumann, M. Schmeisser, J. Völker, P. Kneisel, R. Nietubyc, S. Schubert, J. Smedley, J. Sekutowicz, I. Will, Phys. Rev. ST Accel. Beams 12 (2013) 123402.

[3] A. Lorusso, F. Gontad, E. Broitman, E. Chiadroni, A. Perrone, Thin Solid Films 579 (2015) 50.

[4] J. Smedley, T. Rao, Q. Zhao, J. Appl. Phys. 98 (2005) 043111.

[5] J. Sekutowicz, J. Iversen, D. Klinke, D. Kostin, W. Möller, A. Muhs, P. Kneisel, J. Smedley, T. Rao, P. Strzyzewski, Z.Li, K. Ko, L. Xiao, R. Lefferts, A. Lipski, M. Ferrario, Proc. of PAC07, Albuquerque, USA 2007, TUPMN021.

[6] F. Gontad, A. Perrone, Nucl. Instr. Meth. Phys. Res. A 747 (2014) 1.

[7] A. Lorusso, A. Cola, F. Gontad, I. Koutselas, M. Panareo, N.A. Vainos, A. Perrone, Nucl. Instr. Meth. Phys. Res. A 724 (2013) 72.

[8] H. Padamsee, Supercond. Sci. Technol. 14 (2001) R28.

[9] M. Krishnan, E. Valderrama, B. Bures, K. Wilson-Elliott, X. Zhao, L. Phillips, A.-M. Valente-Feliciano, J. Spradlin, C. Reece, K. Seo, Supercond. Sci. Technol. 24 (2011) 115002.

[10] G. Pristàš, S. Gabáni, E. Gažo, V. Komanický, M. Orendáč, H. You, Thin Solid Films 556 (2014) 470.

[11] R. Banerjee, E.A. Sperling, G.B. Thompson, H.L. Fraser, S. Bose, P. Ayyub, Appl. Phys. Lett. 82 (2003) 4250.

[12] J. Spradlin, A.-M. Valente-Feliciano, H.L. Phillips, C.E. Reece, X. Zhao, D. Gu, K. Seo, Proc. of SRF2011, Chicago, USA 2011, THPO064.

[13] Q. Liu, L. Zhang, L. Cheng, J. Liu, Y. Wang, Appl. Surf. Sci. 255 (2009) 8611.

[14] O. Hellwig, H. Zabel, Physica B 283 (2000) 228.

[15] Th. Proslier, Y. Ha, J. Zasadzinski, G. Ciovati, P. Kneisel, C. Reece, R. Rimmer, A. Gurevich, L. Cooley, G. Wu, M. Pellin, J. Norem, J. Elam, C. Antoine, Proc. of PAC09, Vancouver, BC, Canada, TU5PFP002.

[16] X. Zhao, A.-M. Valente-Feliciano, C. Xu, R.L. Geng, L. Phillips, C.E. Reece, K. Seo, R. Crooks, M. Krishnan, A. Gerhan, B. Bures, K. Wilson Elliot, J. Wright, J. Vac. Sci. Technol. A 27 (2009) 620.

[17] H. Ji, G.S. Was, J.W. Jones, N.R. Moody, J. Appl. Phys. 81 (1997) 6754.
[18] F. Gontad, A. Lorusso, L. Solombrino, I. Koutselas, N. Vainos, A. Perrone, J. Mater. Sci. Technol. 31 (2015) 784.
[19] PDF card no. 34-0370, JCPDS-International Centre for Diffraction Data, 2000.
[20] PDF card no. 35-0789, JCPDS-International Centre for Diffraction Data, 2000.
[21] PDF card no. 04-0686, JCPDS-International Centre for Diffraction Data, 2000.
[22] B. Okolo, P. Lamparter, U. Welzel, E.J. Mittemeijer, J. Appl. Phys. 95 (2004) 466.
[23] "Deposition of Niobium on Silicon through PLD at different substrate temperatures" In preparation
[24] K. Kese, Z. Li, Scripta Mater. 55(8) (2006) 699.
[25] A. M. Korsunsky, A. Constantinescu, Mat. Sci.Eng. A-Struct. 423 (2006) 28.
[26] Y. Zhao and W. Lai, Acta Metall. Sin. 25(2) (2012) 141.
[27] E Bemporad, F Carassiti, M Sebastiani, G Lanza, V Palmieri and H Padamsee, Supercond. Sci. Technol. 21 (2008) 125026.
[28] J.B. Miller, H.-J. Hsieh, B. H. Howard, E. Broitman, Thin Solid Films 518 (2010) 6792.
[29] B.T. Matthias, T.H. Geballe, V.B. Compton, Rev. Mod. Phys. 35 (1963) 1.
[30] J. Eisenstein, Rev. Mod. Phys. 26(3) (1954) 277.

Table I. Experimental conditions

Target		Nb
Substrate		Pb
Substrate temperature		300 K
Target–substrate distance		5 cm
Laser spot size		1.4 mm
Laser pulse duration		7 ns
Laser fluence		8.5 J/cm^2
Power density		1.2 GW/cm^2
Laser wavelength		266 nm
Background pressure		2.2×10^{-6} Pa
Laser shots	Cleaning	3×2,000 per track
	Deposition	3×20,000 per track
Average number of pulses/site		700
Film thickness		60 nm

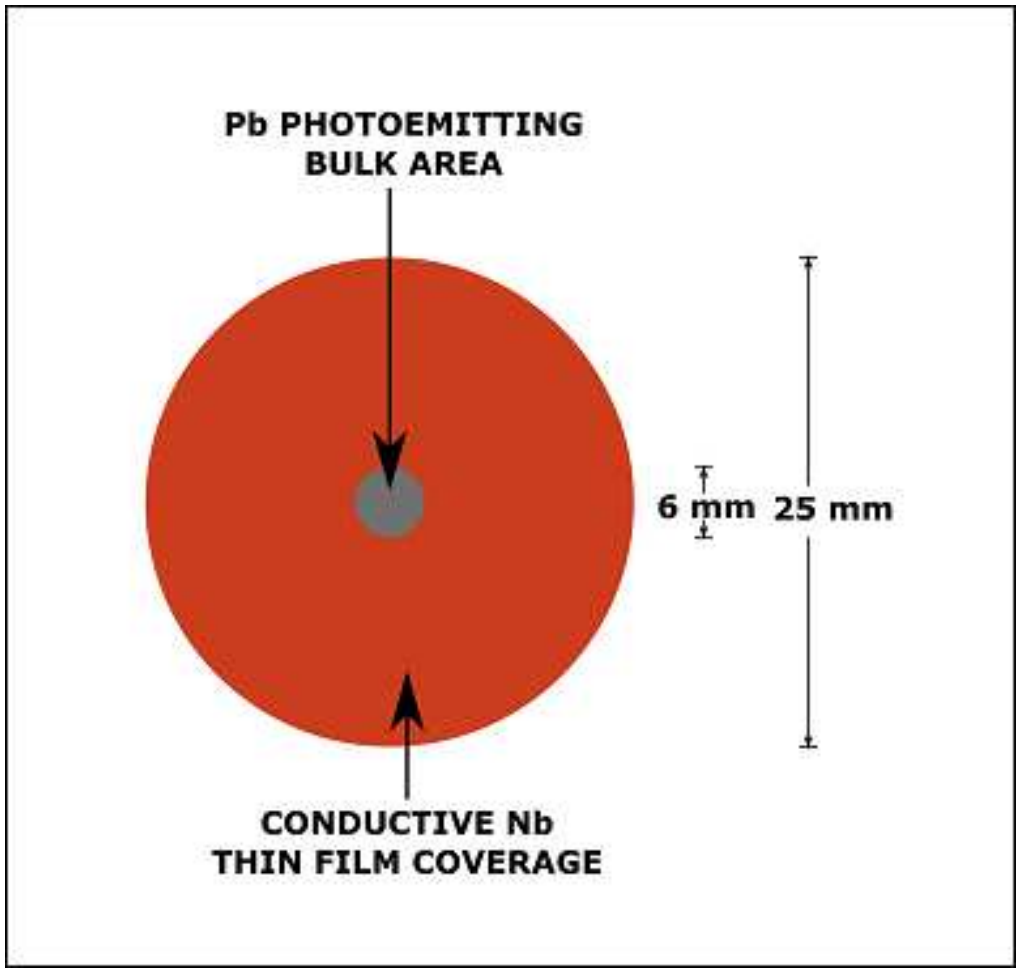

Figure 1

Scheme of the annular photocathode configuration. The central part of the cathode corresponds to the Pb photoemitting area while the external area is the Nb superconducting deposited film.

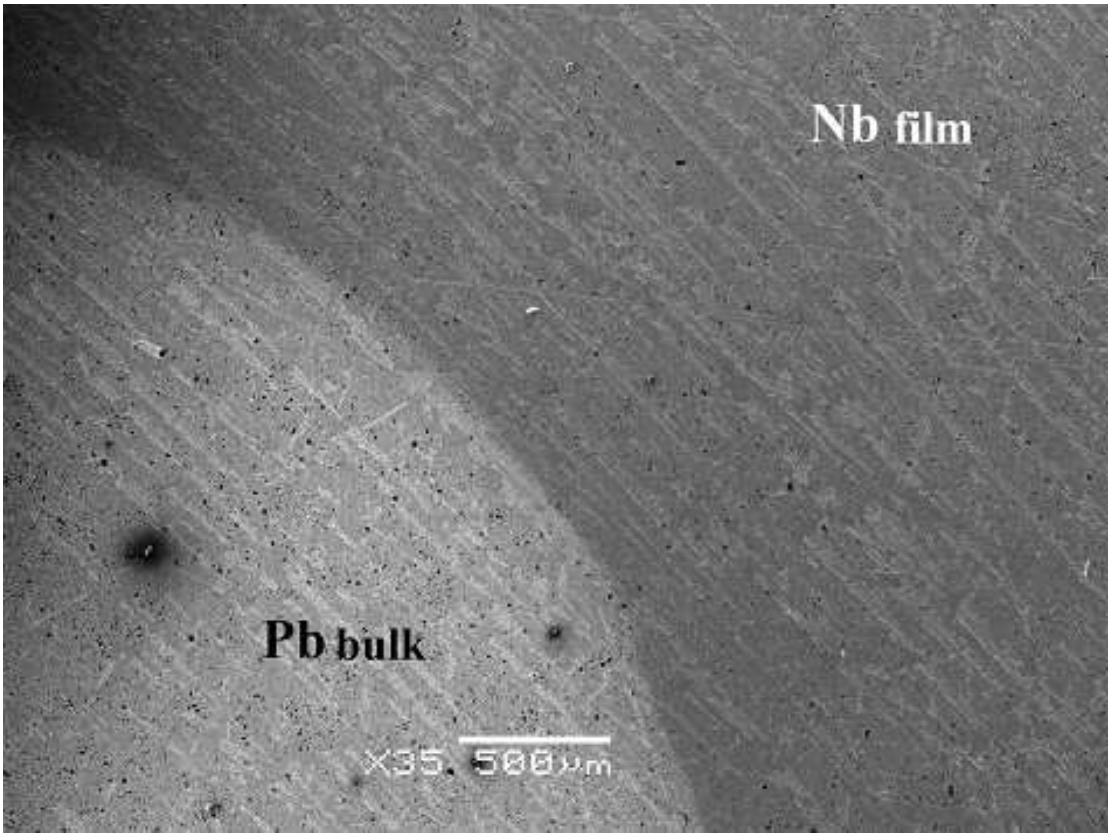

Figure 2

SEM micrograph of the cathode. The darker area corresponds to the Nb coating. The circular brighter area corresponds to the photoemitting spot.

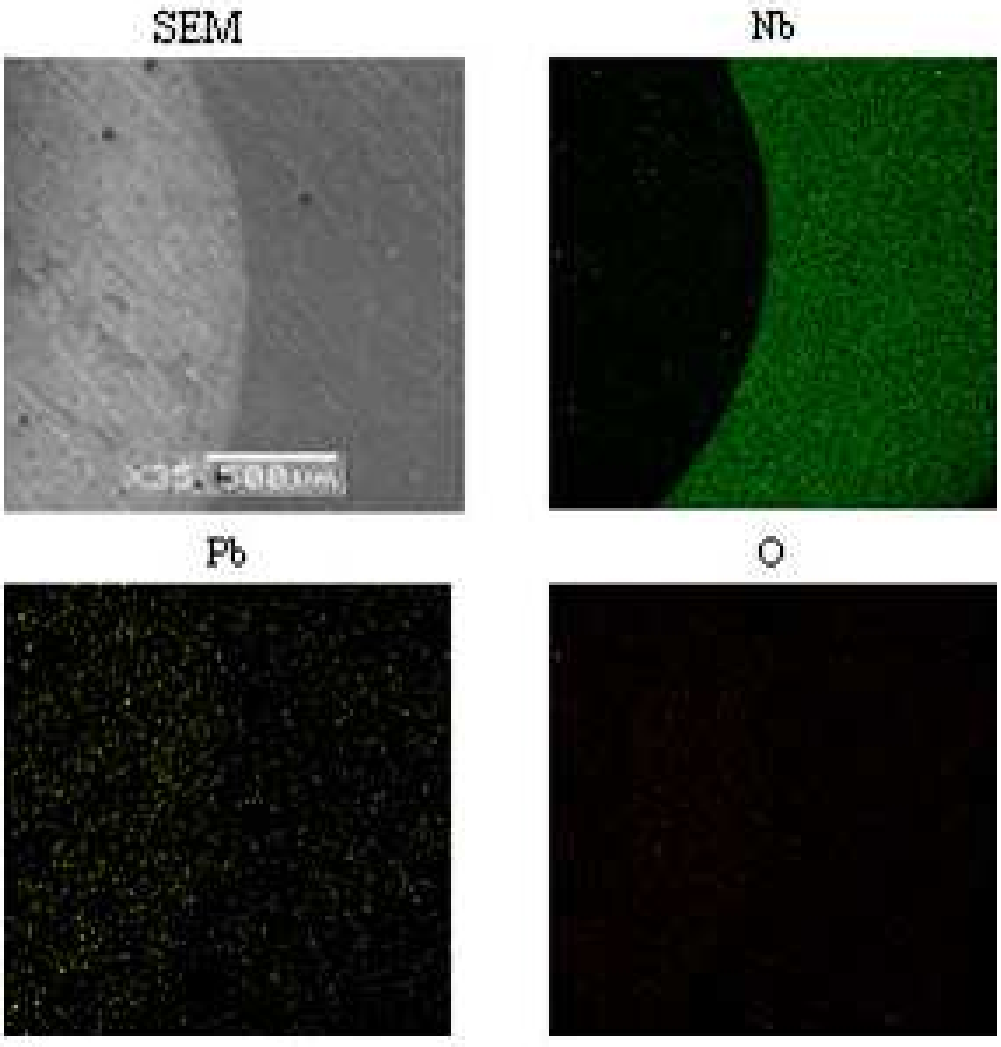

Figure 3

SEM image and EDX maps of the cathode obtained with electron energy of 15 keV.

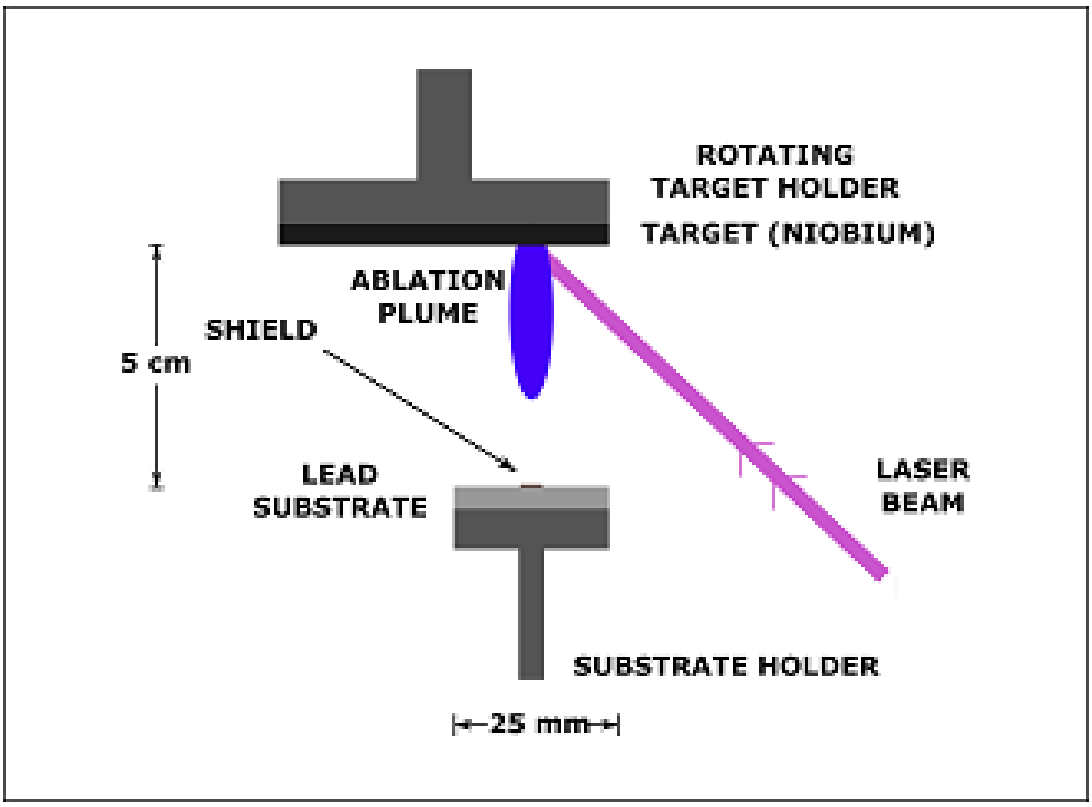

Figure 4

Schematic of the geometrical configuration of the experimental setup for the deposition of the Nb films.

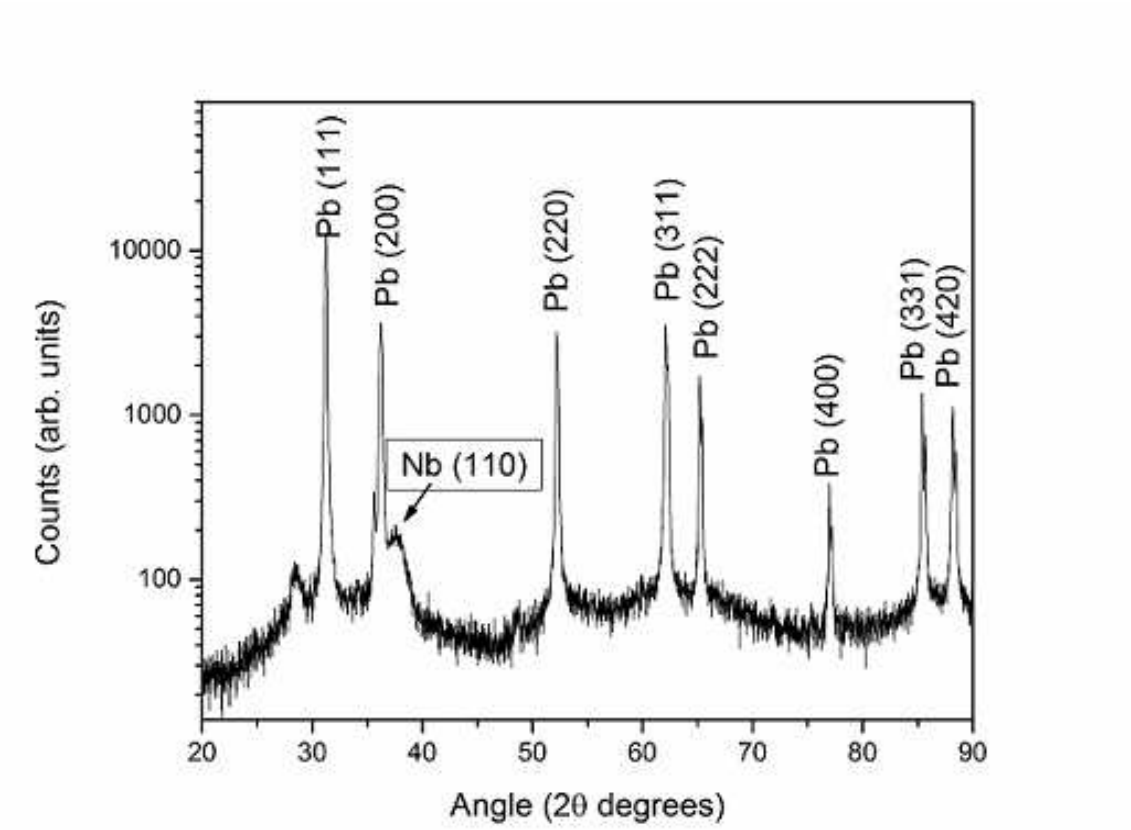

Figure 5

θ–2θ XRD pattern of the Nb film on the Pb substrate. Peaks corresponding to the different crystalline orientations of Nb are evident [19, 20] as well as the peaks corresponding to the Pb polycrystalline substrate [21].

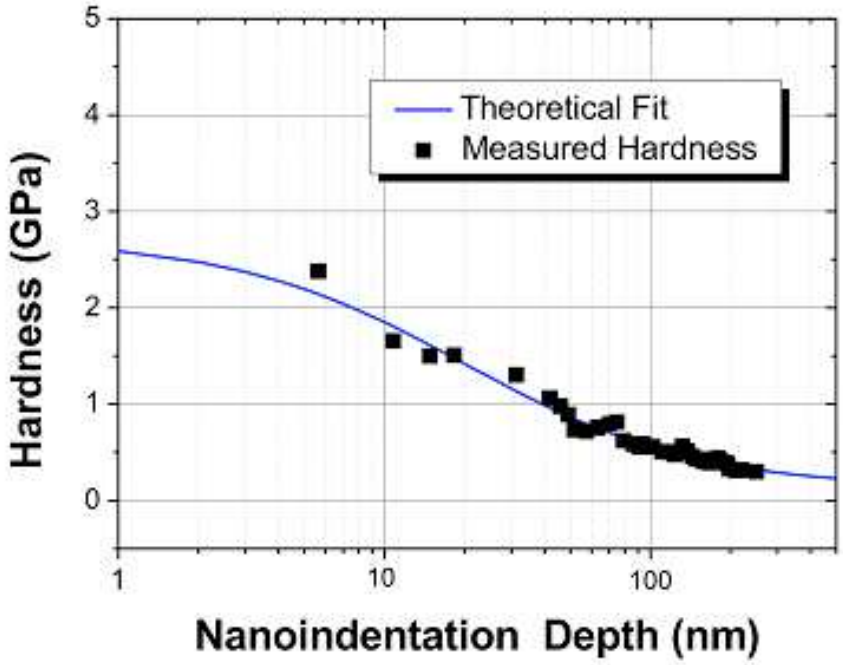

Figure 6

Hardness as a function of indenter displacement for a thin Nb film deposited on a Pb substrate. The continue line is the fit curve obtaining the indentation response function of Eq. 1

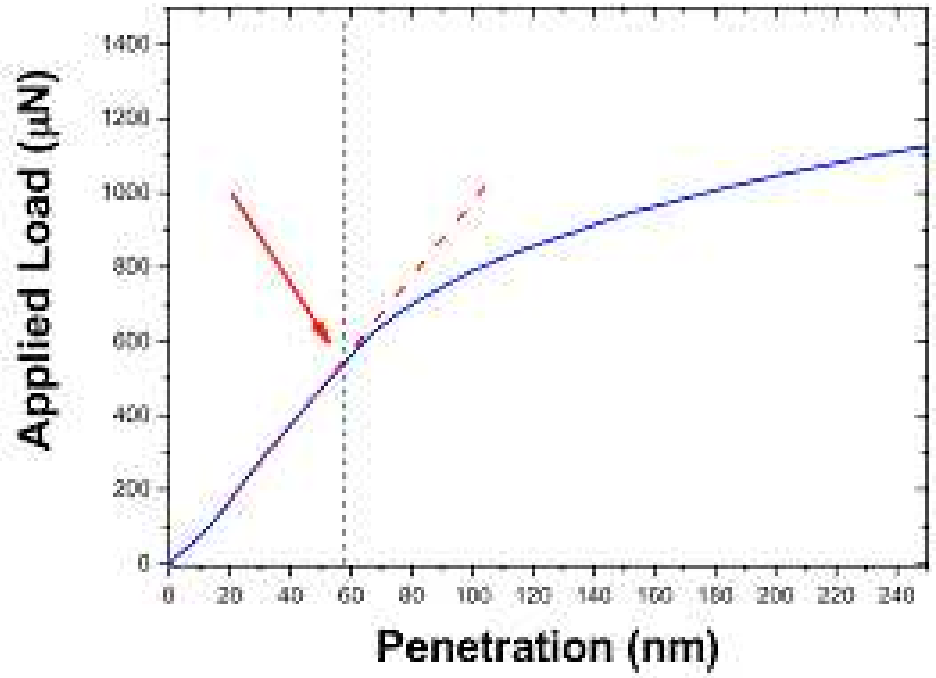

Figure 7

Load-displacement curve of the nanoindentation probe. The arrow shows the place where the curve has a change in the slope, indicating that the material gets softer at about 60 nm from the surface.

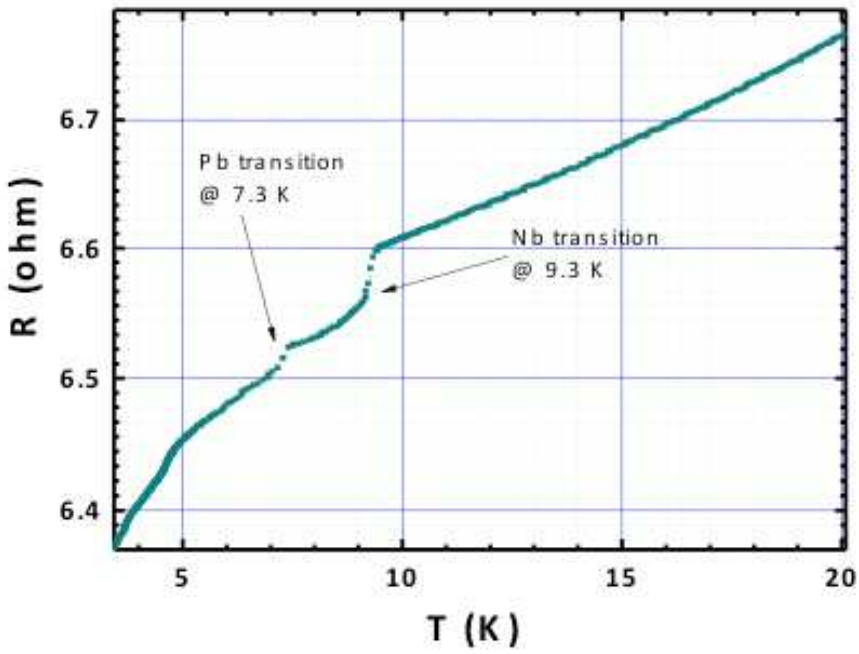

Figure 8

Evolution of the sample electrical resistance with the temperature.